



*Supplement of*

## **Solar irradiances measured using SPN1 radiometers: uncertainties and clues for development**

**J. Badosa et al.**

*Correspondence to:* J. Badosa (jordi.badosa@lmd.polytechnique.fr)

## S Supplementary material

### S.1 Case studies

Figures S1, S2 and S3 show three case study examples for Palaiseau with diurnal cycle where TSI images are available:

- Day **20110323**: Cloudless day with large aureole energy due to an important aerosol load (AOD at 500 nm of 0.2 in the morning and increasing to 0.3 in the afternoon). This is a good example of the azimuth effect seen in Fig. 8.
- Day **20110301**: The same effect (but larger) is seen in this case caused by the presence of bright clouds around the sun.
- Day **20110227**: Day with mainly broken clouds passing (and cirrus appearing at the end of the afternoon) that lead to moments with almost cloudless, sky heterogeneous radiance and nearly overcast conditions. Consequently, quite diverse DHI SPN1-TBM difference values are found, from -50 to + 50 W/m<sup>2</sup>.

### S.2 Polar plots for GHI and DNI SPN1-TBM

Figures S4 and S5 show GHI and DNI SPN1-TBM differences as a function of SZA and SAA.

### S.3 Other factors affecting accuracy

#### S.3.1. Thermal effects

The dominant thermal effect for the SPN1 is a sensitivity to changing temperatures, of around 3W/m<sup>2</sup> at 5°C/Hr. This can be seen over the course of the day as a small negative error in the morning as temperatures rise, and a small positive error as temperatures fall. This is visible in Figs 8 and 10 as a slope in the general trend from East (SAA=90°) to West (SAA=270°). This effect is also responsible for some of the shorter-timescale variability in SPN1 Diffuse and Global outputs during the day, as it responds to small changes in heat load due to changing solar radiation or atmospheric turbulence.

Figure S6a shows these offsets due to large temperature changes measured in an environmental chamber. The temperature was progressively changed from a starting point

of 20°C up to 60°, down to -20°C and back to 20°C, with a repeating pattern of holding the temperature constant for 1 hour, then a change of 20° over 1 hour.

Readings from the individual detectors were recorded, against a constant light level of 19 W.m-2. Figure S6a shows that the thermopile outputs are lowered during periods of rising temperature, and increased during periods of falling temperatures, and return to the 19 W.m-2 reference value when the temperature stabilizes. The amount of the deviation is up to 6W.m-2 (in the individual thermopile readings) for a temperature change of 20°C Hr-1. This will be doubled in calculating the GHI & DHI outputs, and is consistent with the specified sensitivity of 3W/m<sup>2</sup> at 5°C/Hr. The sensitivity to changing temperature is largely independent of the actual temperature value.

Figure S6b shows the SPN1 DHI measurements during a very clear day at Palaiseau at 1 min averages. The SPN1 internal temperature was also measured, and the change in temperature over 2 minutes is also shown. Close inspection shows a high correlation between the SPN1 rate of temperature change and the short-term DHI variability. Early morning and late afternoon temperature corrections are also seen in Fig. S6b due to temperature increasing and decreasing, respectively. The measured temperature change can be used to correct the SPN1 readings using the sensitivity to temperature change shown in Fig. S6A, and produces a smoother DHI measurement. This variation might also be improved by some additional shielding around the SPN1.

The SPN1 thermopiles are protected from longwave I-R radiation by a sapphire window, the diffuser material, and finally a glass dome. This means that there is no apparent sensitivity to longwave IR changes (which result in the usual negative night-time readings for pyranometers).

### S.3.2. Electrical effects

The internal electronics of the SPN1 are only capable of positive values, and cannot at any point go below 0V. In addition to this, there is a small amount of noise present in the sensor measurements, giving a small positive reading. The analogue output Digital to Analogue Convertors typically also have a small positive offset. The combination of these factors produces a reading of 1-3 W.m<sup>-2</sup> in dark conditions, whereas pyranometers often have a similar sized negative output in dark conditions as they are sensitive to the longwave IR radiation flux from the instrument toward the sky. These two offsets combine to produce a typical offset of around 5W.m-2 between SPN1 and pyranometer outputs. These offsets will generally also be present during the day, though hidden by the daylight values (Vignola et al, 2012).

Figure S6c shows typical night-time values for a range of different pyranometers and SPN1s over several nights. This is shown as hourly averages to clearly separate the traces.

- Red/brown traces are SPN1s
- Blue traces are unheated, unventilated CMP11/21 type pyranometers
- Green traces are ventilated, heated CMP6 type pyranometers.

### S.3.3. Time response

The SPN1 thermopiles have a very fast response (100ms typically) compared with pyranometers (3s – 30s typically). This will produce an increased scatter in comparisons of 1-minute or faster datasets due to the difference in response times.

### **S.3.4. Soiling, rain, frost, snow**

The internal heater of the SPN1 appears to have a similar effectiveness to a heater/ventilator unit on a pyranometer, and keeps the SPN1 dome clear of rain, dew, frost and snow under most conditions.

Fig S6d shows two adjacent SPN1s at Palaiseau after a rain shower – one (in the background to the right) with the heater connected, the other (in the foreground) not connected. The heated SPN1 dome is cleared of raindrops very much quicker than the unheated one. The lower image shows the effectiveness of the heater in frost and snow (from Matsui et al, 2012).

## **S.4 Detailed explanation of SPN1 internal calculations.**

The standard SPN1 internal software contains some additional corrections compared with the basic algorithm presented in Sect. 1. The detailed algorithm and reasons for the various corrections is presented below (based on the SPN1 User manual).

Let MAX and MIN be the largest and smallest thermopile readings of the seven thermopiles, after being adjusted for individual thermopile calibration factors (calibration is done in the solar lamp integrating sphere against a transfer standard SPN1)

Then  $GHI = MAX + MIN$

$DHI = 2 * MIN * 1.02$  (the extra 2% takes away a small systematic bias due to there being typically a 1%-2% spread between sensors under identical lighting conditions).

IF  $(DHI > GHI)$  then  $DHI = GHI$  (a sanity check as Diffuse obviously can't ever be greater than Global in reality)

There is then a further correction due to the spectral response of the sensors giving a different sensitivity to direct and diffuse light in most conditions:

$BHI = (GHI - DHI) * 0.99$  (because the direct beam usually has less red than GHI, so is overmeasured)

$DHI = DHI * 1.14$  (corrects for the overall slope of the points in a graph such as Fig.6b)

$GHI = BHI + DHI$ . (GHI & DHI are output)

## **S.5 Dome lensing effect diagram**

Figure S.7 shows ray traces of parallel rays from the sun incident on the SPN1 detectors, showing the effects of refraction by the glass dome. The effect of this is that the detector furthest from the sun (on the left side of the diagram) absorbs a slightly smaller part of the solar beam than the detector closer to the sun (on the right side of the diagram).

## **S.6 Diffuse first touch angle diagram**

The diagram shows a projection of the 7 detectors onto the shadowmask in the direction of the sun (dark ovals). For the fully shaded detectors, the largest possible cone directed towards the sun that is still fully shaded is drawn (red circles). The half-angle of this cone gives the first touch angle for the detector – in this case  $4^\circ$  for detector 4,  $12^\circ$  for detector 7. The largest first touch angle is taken as the diffuse first touch angle for the given solar position, in this case  $12^\circ$ . The solar aureole out to  $12^\circ$  will be wholly excluded from the diffuse measurement in this case.

## **S.7 References**

Matsui, N., C. Long, J. Augustine, D. Halliwell, T. Uttal, D. Longenecker, O. Nievergall, J. Wendell, and R. Albee (2011), Evaluation of arctic broadband surface radiation measurements, *Atmospheric Measurement Techniques Discussions*, 4(4), 4911-4936.

Vignola, F., Michalsky, J., & Stoffel, T. (2012). Solar and infrared radiation measurements. CRC Press.

## Figures of the Supplementary Material

## Figure S1 case study 1

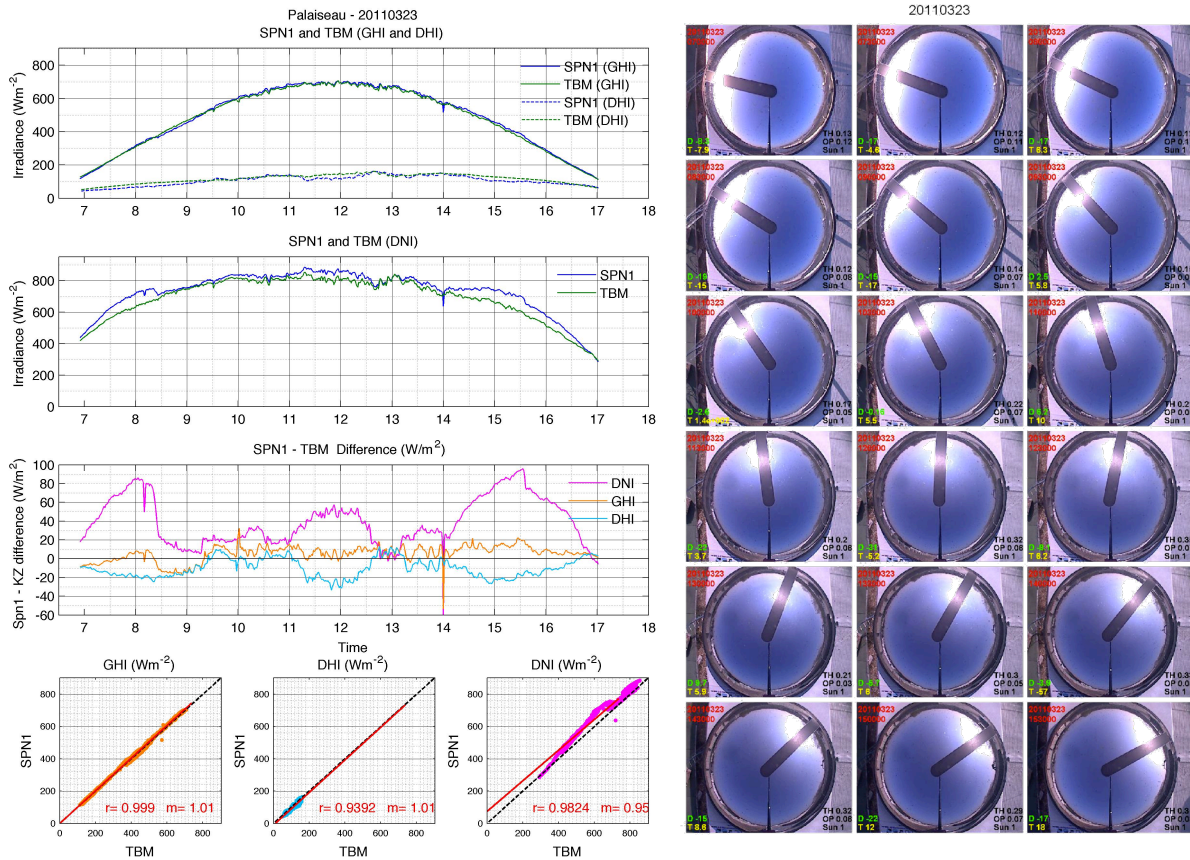


## Figure S2 case study 2

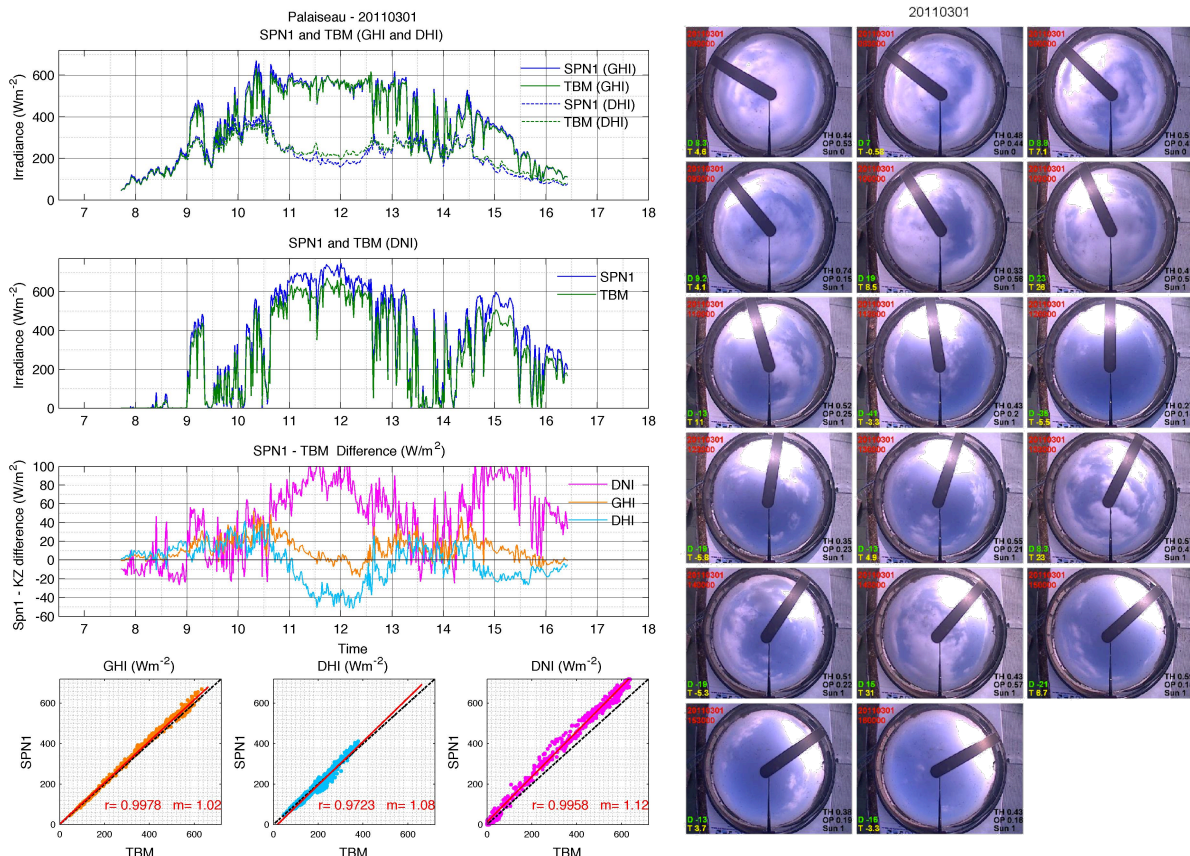


Figure S3 case study 3

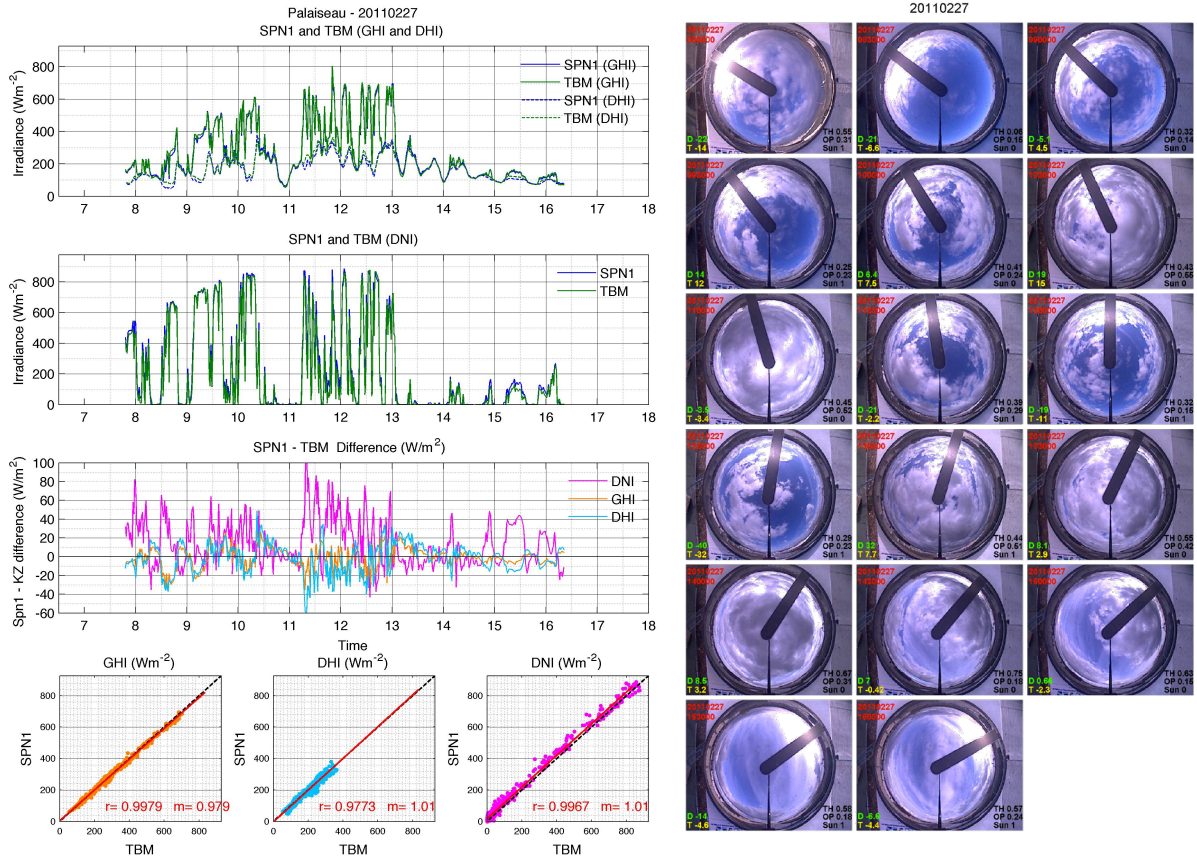


Figure S4 –GHI differences (TBM– SPN1) in polar coordinates (of SZA and SAA). SPN1 values have been re-calibrated as described in Sect. 4.2.

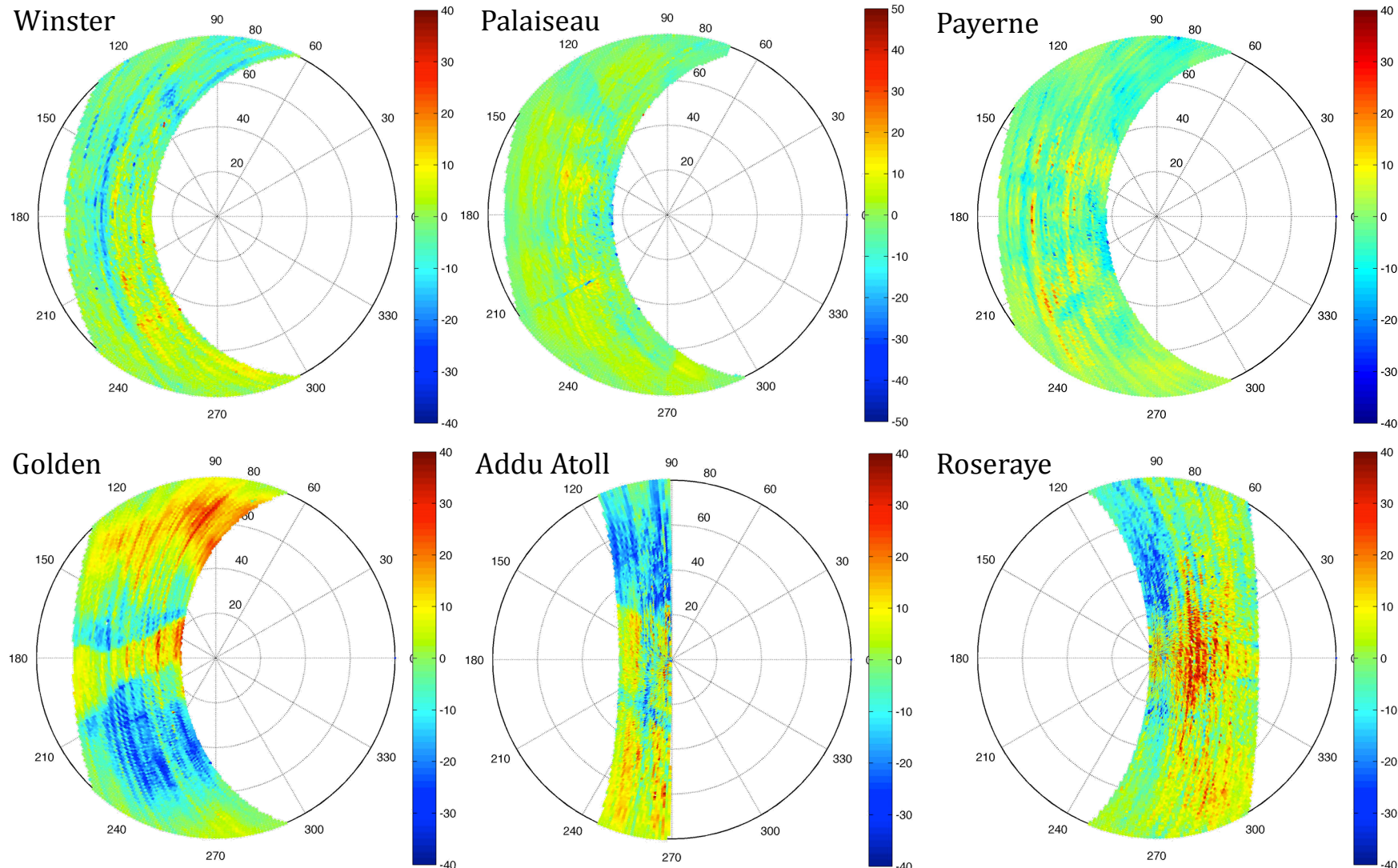


Figure S5 – Same as Figure S4 for DNI differences (TBM– SPN1) in polar coordinates (of SZA and SAA). White regions inside red regions are related to DNI differences > 80 W/m<sup>2</sup>, which are left out of the plot (to keep color contrast).

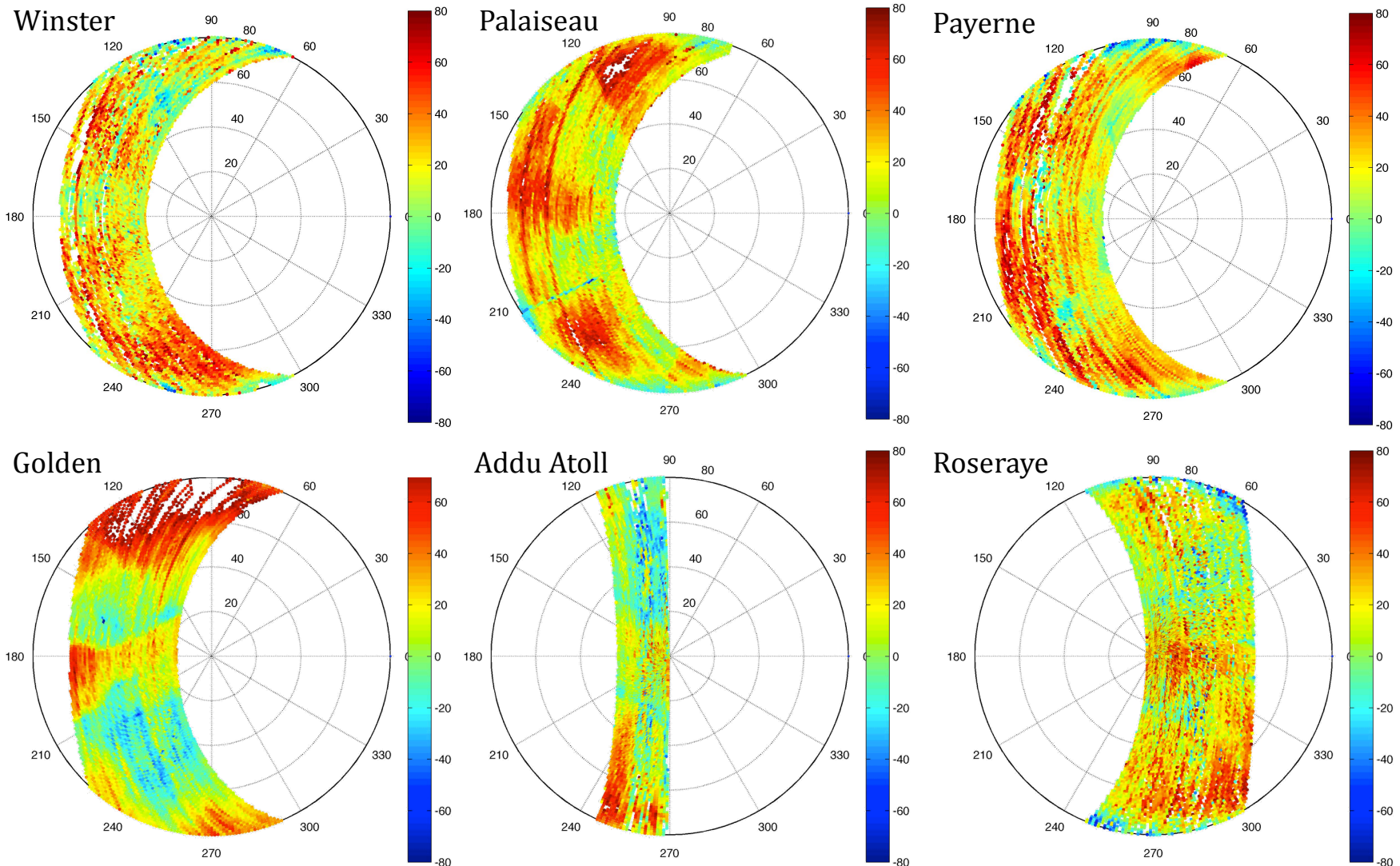
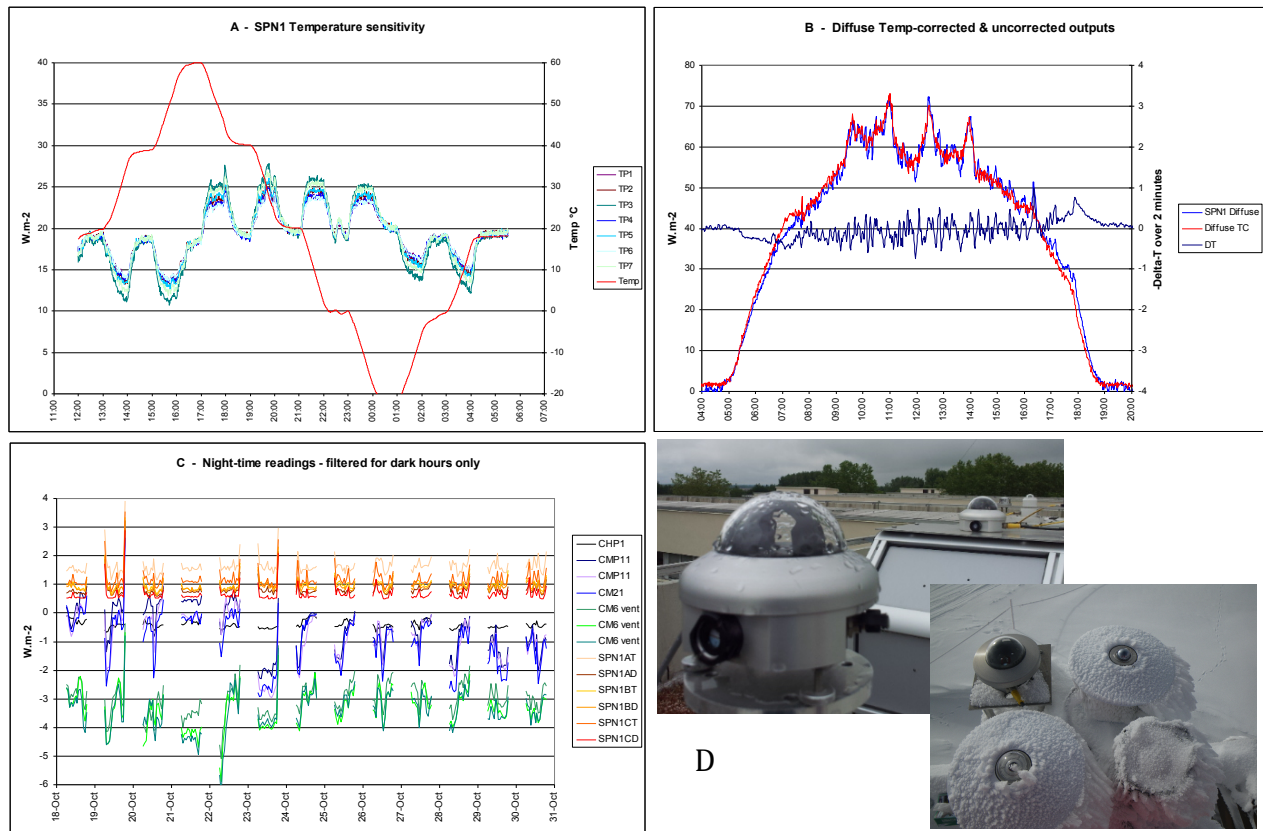
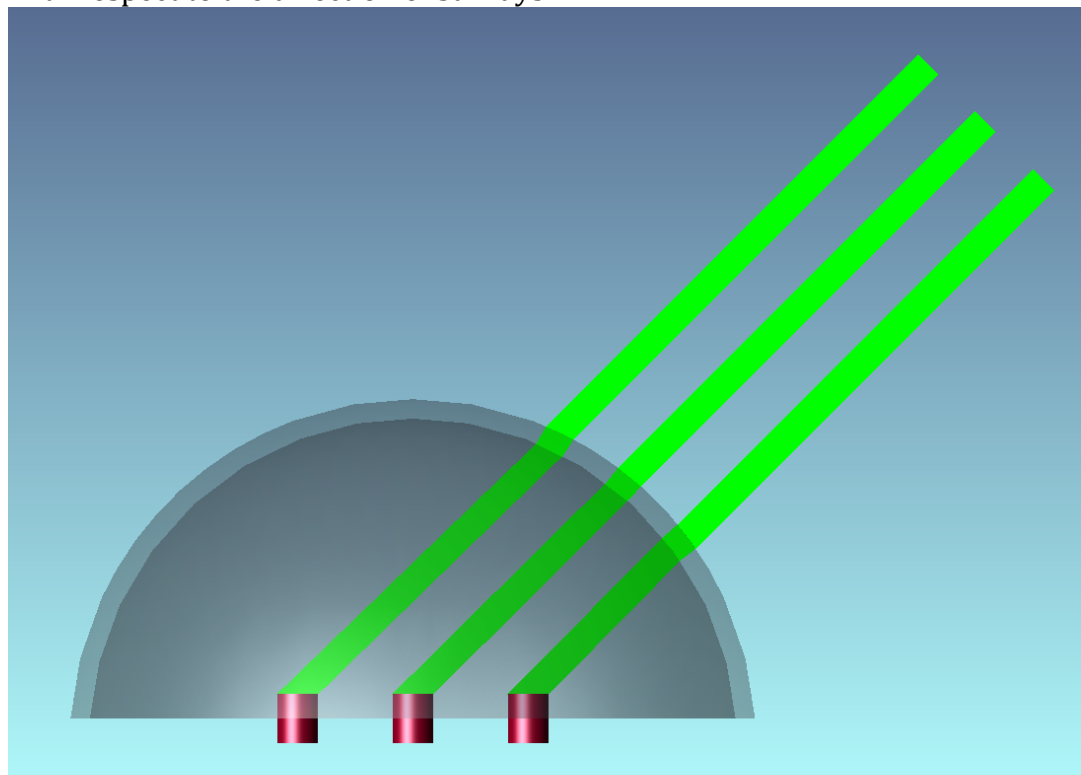


Figure S6 – temperature & thermal effects



S.7 Diagram showing the dome lensing effect on SPN1 sensors depending on their position with respect to the direction of sunrays.



S.8 Diagram showing an example for the diffuse first touch angle definition (see explanations in sections 5.2.3 and S.6).

